

CONSTRUCTING CONTROL LANDSCAPE FOR NON-CONVEX OPTIMAL CONTROL OF ELLIPTIC EQUATION BY PDE-CONSTRAINED HIGH-INDEX SADDLE DYNAMICS*

NING DU[†], YANLIN LIU[†], LEI ZHANG[‡], AND XIANGCHENG ZHENG[†]

Abstract. Non-convex optimal control arises from various applications but may contain multiple stationary points. Classical solvers usually perform a “local” search near a saddle point or a local minimum, thus rely on good initial guess to reach the (quasi-)optimal control. We introduce a novel solution strategy for the non-convex optimal control of an elliptic equation. We develop a PDE-constrained high-index saddle dynamics (PCHiSD) to construct the control landscape. This method depicts the macroscopic configuration of control and state spaces such that the local and global minima could be systematically computed along the transition pathways in control landscape without requiring good initial conditions. We establish the well-posedness of the state equation and the existence of an optimal control, and then implement the PCHiSD and control landscape algorithms for numerical experiments and comparisons. Numerical results not only indicate the effectiveness of the proposed method, but reveal unintuitive phenomena that supports the necessity of computing multiple solutions of high indices.

Key words. non-convex, optimal control, high-index saddle dynamics, control landscape, multiple solutions

MSC codes. 49M41, 65K10, 65N06

1. Introduction.

1.1. Motivations and ideas. Non-convex optimal control is widespread in scientific and engineering problems [1, 20], and extensive numerical methods have been developed, including the gradient and Newton-type methods [18, 23, 24], the sequential quadratic programming [24], the penalized gradient projection method [8, 11], the semismooth Newton method [19, 21], and the neural network approach [12]. Nevertheless, most methods perform a “local” study without considering the macroscopic configuration. Specifically, they usually focus on investigations of a saddle point or local minimum of the non-convex optimal control, and rely on good initial conditions to reach the (quasi-)optimal minima. To address these issues, this work intends to propose a novel solution strategy based on systematic saddle point algorithms, which investigates the non-convex optimal control from a comprehensive and global perspective without requiring good initial guesses.

For clarity, we first introduce several concepts. For a twice Fréchet differentiable energy functional $E(x)$ with $x \in \mathbb{R}^m$ ($m \in \mathbb{N}^+$), a stationary point x^* of E satisfies $\nabla E(x^*) = 0$. If x^* is not a minimum, then we call x^* a saddle point. The Morse index of a nondegenerate saddle point is the maximal dimension of a subspace on which its Hessian is negative definite [22], and we call a saddle point with Morse index k an

*Submitted to the editors DATE.

Funding: This work was partially supported by the National Key R&D Program of China (No. 2023YFA1009200, 2023YFA1008903), the National Natural Science Foundation of China (No. 12225102, T2321001, 12288101, 12301555, 12131014), the Natural Science Foundation of Shandong Province (No. ZR2025QB01), the Taishan Scholars Program of Shandong Province (No. tsqn202306083).

[†]School of Mathematics, Shandong University, Jinan, 250100, China (Emails: duning@sdu.edu.cn, yanlinliu@mail.sdu.edu.cn, xzheng@sdu.edu.cn).

[‡]Beijing International Center for Mathematical Research, Center for Machine Learning Research, Center for Quantitative Biology, Peking University, Beijing, 100871, China (Email: zhangl@math.pku.edu.cn).

index- k saddle point (a minimum is indeed an index-0 saddle point). There exist several efficient methods for locating saddle points, one of which is the high-index saddle dynamics (HiSD) method [29]. With the help of HiSD, the solution landscape method, which aims to construct a pathway map containing saddle points and local minima of a system and the connections among them, has been developed in [28] and successfully applied in several fields [25–27]. A typical procedure to construct the solution landscape starts from a high-index saddle point (i.e. the parent state) and then locates lower-index saddle points by the HiSD [28]. Since the initial values of HiSD for a certain saddle point are provided from eigenvectors of the Hessian at a higher-index saddle point, the solution landscape method circumvents the difficulty of selecting proper initial values and makes the downward search for lower-index saddle points efficient.

Based on the above discussions, we follow the spirit of the solution landscape method to solve the non-convex optimal control. Nevertheless, there are substantial differences from solving energy functionals in the literature. For instance, the traditional HiSD relies on the explicit expression of the gradient of the model, which could be simply obtained from the given energy functional. However, for PDE-constrained optimal control problems, evaluating the gradient of the cost functional is not straightforward due to the implicit dependence of the state variable on the control variable via the state equation. Thus, novel multiple solution algorithms need to be developed for PDE-constrained non-convex optimal control problems.

1.2. Non-convex optimal control model. In this work, we demonstrate the novel solution strategy of non-convex optimal control by the following problem

$$(1.1) \quad \min_{u \in \mathbb{H}^1(\Omega)} J(y, u) := \frac{1}{2} \|y - y_d\|_{\mathbb{L}^2(\Omega)}^2 + \frac{\lambda}{2} \|u\|_{\mathbb{H}^1(\Omega)}^2,$$

subject to a general elliptic equation with nonlinear mappings on both y and u (cf. [4, 6] for similar nonlinear state equations in optimal control)

$$(1.2) \quad \begin{cases} \mathcal{A}y + d(x, y) = g(x, u) & \text{in } \Omega, \\ y = 0 & \text{on } \Gamma. \end{cases}$$

Here $\Omega \subset \mathbb{R}^n$ ($1 \leq n \leq 3$) is a bounded domain with a $\mathbb{C}^{1,1}$ boundary Γ , and y and u denote the state and control variables, respectively. The spaces $\mathbb{L}^q(\Omega)$ and $\mathbb{H}^q(\Omega) := \mathbb{W}^{2,q}(\Omega)$ for $1 \leq q \leq \infty$ denote the standard Lebesgue and Sobolev spaces, respectively, equipped with standard norms. The $y_d(x)$ denotes the desired state and $\lambda > 0$ is the regularization parameter. In the state equation, \mathcal{A} is a symmetric and coercive second-order elliptic operator

$$\mathcal{A}y(x) := - \sum_{i,j=1}^n \partial_{x_i} (a_{ij}(x) \partial_{x_j} y(x)) + c(x)y(x),$$

where $a_{ij}(x) \in C^1(\overline{\Omega})$, the space of continuously differentiable functions on $\overline{\Omega}$, $c(x) \in \mathbb{L}^\infty(\Omega)$, and $d(x, y)$ and $g(x, u)$ are given functions. In this work, we mainly consider the unconstrained case, that is, there is no additional constraint for $u \in \mathbb{H}^1(\Omega)$. In Section 3.4 and numerical experiments, we discuss the integral constrained case.

It is worth mentioning that in most studies the \mathbb{L}^2 regularization is adopted since it suffices to ensure the well-posedness of the optimal control [7, 16]. To accommodate the non-convexity of the cost function arising from the nonlinearity of the state equation,

we instead apply the \mathbb{H}^1 regularization to further penalize the gradient, which not only appears in several circumstances such as switching control [9, 10], optimal control with complementarity constraints [14, 17] and optimal control of elliptic problems [2, 13], but could suppress excessive oscillations on the control caused by, e.g. the non-convexity of the cost function.

1.3. Contributions of the work. The main contributions of the work are enumerated as follows:

- For optimal control (1.1)–(1.2), we prove the well-posedness of the state equation and the existence of an optimal control. The analysis differs from the existing ones in the literature in that more subtle analysis is performed within the classical framework of the existence proof to accommodate the nonlinear mapping of the control variable.
- We design a PDE-constrained HiSD (PCHiSD) to locate saddle points of the non-convex optimal control problem (1.1)–(1.2), which accommodates the effects of state equation by means of adjoint equation such that it has substantial differences from the traditional HiSD and is particularly suitable for PDE-constrained multiple solution problems. We also extend this algorithm to the case with integral constraint on the control variable. Traditionally such constraints are usually preserved by involving them in the first-order optimality conditions. In this work, we alternatively preserve the integral constraint by restricting the PCHiSD on the appropriate manifold, which results in a projected PCHiSD. A main advantage lies in the efficient implementation by circumventing the first-order optimality conditions.
- By PCHiSD, we construct the control landscape for non-convex optimal control (1.1)–(1.2), and then find saddle points and minima along the transition pathways. Compared with traditional optimization algorithms such as the gradient method and the Newton's method, the control landscape method provides a systematic approach for locating local and global minima without requiring good initial guesses. Furthermore, we find from the control landscape that in some complex examples the values of J at some lower-index saddle points are higher than those at their adjacent higher-index saddle points, which is nonintuitive and suggests the necessity of computing saddle point solutions in finding the optimal control.

The rest of the paper is organized as follows: In Section 2, we present a detailed analysis of the optimal control problem (1.1)–(1.2). In Section 3, we develop the PCHiSD for unconstrained and constrained optimal control problems and discussion the construction of the control landscape. In Section 4, we perform several numerical experiments and comparisons. Some concluding remarks are addressed in the last section.

2. Analysis of optimal control. This section presents the analysis of the non-convex optimal control problem (1.1)–(1.2). We assume that the semilinear term $d(x, y)$ satisfies standard local Lipschitz continuity and monotonicity, see e.g. the book of Tröltzsch [24, Assumption 4.14]. We also impose local or global Lipschitz continuity (depending on the dimension n of the problem) and growth conditions on $g(x, u)$ to ensure the well-posedness of the state equation.

For $n = 1$, we impose Assumptions A and B as follows:

Assumption A

- (i) $d(\cdot, \cdot) : \Omega \times \mathbb{R} \rightarrow \mathbb{R}$ is a Carathéodory function.

(ii) $d(x, y)$ is twice continuously differentiable with respect to y . There exists a $K > 0$ such that

$$(2.1) \quad |d_y^{(j)}(x, 0)| \leq K, \text{ for } 0 \leq j \leq 1, \text{ and a.e. } x \in \Omega,$$

and for any $E > 0$ there exists a positive constant L_E such that

$$(2.2) \quad |d_y^{(j)}(x, y_1) - d_y^{(j)}(x, y_2)| \leq L_E |y_1 - y_2|, \text{ for } 0 \leq j \leq 1 \text{ and a.e. } x \in \Omega,$$

where $y_i \in \mathbb{R}$ satisfies $|y_i| \leq E$ for $i = 1, 2$ and $d_y^{(j)}$ denotes the j th derivative with respect to y .

(iii) $d_y(x, y) > 0$ for any $y \in \mathbb{R}$ and a.e. $x \in \Omega$.

Assumption B

(i) $g(\cdot, \cdot) : \Omega \times \mathbb{R} \rightarrow \mathbb{R}$ is a Carathéodory function.

(ii) $g(x, y)$ is twice continuously differentiable with respect to u , and for any $M > 0$, there exists a positive constant L_M such that

$$(2.3) \quad |g_u^{(j)}(x, u_1) - g_u^{(j)}(x, u_2)| \leq L_M |u_1 - u_2|, \text{ for } 0 \leq j \leq 1 \text{ and a.e. } x \in \Omega,$$

where $u_i \in \mathbb{R}$ satisfies $|u_i| \leq M$ for $i = 1, 2$.

(iii) There exist a constant $b > 0$ and a function $a \in \mathbb{L}^2(\Omega)$ such that $g(x, u)$ satisfies the growth condition for some $1 \leq s < \infty$

$$|g(x, u)| \leq a(x) + b |u|^s, \text{ for a.e. } x \in \Omega \text{ and any } u \in \mathbb{R}.$$

For $n = 2, 3$, we impose the Assumptions A and C:

Assumption C

(i) $g(\cdot, \cdot) : \Omega \times \mathbb{R} \rightarrow \mathbb{R}$ is a Carathéodory function.

(ii) $g(x, y)$ is twice continuously differentiable with respect to u , and there exists an $L_0 > 0$ such that for any $u_1, u_2 \in \mathbb{R}$

$$|g_u^{(j)}(x, u_1) - g_u^{(j)}(x, u_2)| \leq L_0 |u_1 - u_2|, \text{ for } 0 \leq j \leq 1 \text{ and a.e. } x \in \Omega.$$

REMARK 2.1. We explain why the imposed Lipschitz continuity for g is local for one-dimensional case but global for two- and three-dimensional cases. The cost functional J includes an \mathbb{H}^1 regularization term such that the space of control variable u is naturally selected as $\mathbb{H}^1(\Omega)$. However, the above assumptions on g rely on the pointwise bound of the input u , which could be given by the Sobolev embedding $\mathbb{H}^1(\Omega) \hookrightarrow \mathbb{L}^\infty(\Omega)$ only in the one-dimensional case. Thus it suffices to impose the local Lipschitz condition for the one-dimensional case but the global Lipschitz continuity is required for two- and three-dimensional cases. Nevertheless, the global Lipschitz continuity may be avoided for some special cases. For instance, if $\lambda = 0$ and a pointwise box constraint on the control variable is imposed, it suffices to impose the local Lipschitz continuity for any dimension, as investigated in [6].

In the rest of this section we analyze the optimal control (1.1)–(1.2) for the one-dimensional case (i.e. $n = 1$) under Assumptions A and B. The two- and three-dimensional problems can be analyzed in a similar and simpler manner under Assumptions A and C due to the global Lipschitz continuity of g , and we thus omit the details of the proofs. We will use C to denote a generic positive constant that may assume different values at different occurrences, and we use $C(M)$ with some quantity M to show the dependence of C on M .

2.1. Well-posedness of state equation. To facilitate the treatment of the nonlinear term $g(x, u)$, we introduce the associated Nemytskii operator \mathcal{G} defined by $\mathcal{G}(u)(x) = g(x, u(x))$ for a.e. $x \in \Omega$. The following lemma describes some properties of \mathcal{G} .

LEMMA 2.1. *Under Assumption B for one-dimensional case (or Assumption C for two- and three-dimensional cases), $\mathcal{G}(u) \in \mathbb{L}^2(\Omega)$ for $u \in \mathbb{H}^1(\Omega)$ and the following estimate holds for some $1 \leq s < \infty$ given in Assumption B in the one-dimensional case or $s = 1$ for two- and three-dimensional cases*

$$\|\mathcal{G}(u)\|_{\mathbb{L}^2(\Omega)} \leq C(1 + \|u\|_{\mathbb{H}^1(\Omega)}^s),$$

where C is independent of u .

Furthermore, for any $M > 0$, the following estimate holds for $u_i \in \mathbb{H}^1(\Omega)$ ($i = 1, 2$) with $\|u_i\|_{\mathbb{H}^1(\Omega)} \leq M$

$$(2.4) \quad \|\mathcal{G}(u_1) - \mathcal{G}(u_2)\|_{\mathbb{L}^2(\Omega)} \leq C(M) \|u_1 - u_2\|_{\mathbb{L}^2(\Omega)}.$$

Proof. We first consider the one-dimensional case. For every control $u \in \mathbb{H}^1(\Omega)$ and a.e. $x \in \Omega$, we have

$$\|\mathcal{G}(u)\|_{\mathbb{L}^2(\Omega)}^2 \leq \int_{\Omega} (a(x) + b|u|^s)^2 dx \leq C(1 + \|u\|_{\mathbb{L}^{2s}(\Omega)}^{2s}) \leq C(1 + \|u\|_{\mathbb{H}^1(\Omega)}^{2s}),$$

where the Sobolev embedding $\mathbb{H}^1(\Omega) \hookrightarrow \mathbb{L}^\infty(\Omega)$ for $n = 1$ is used. Give any $M > 0$ and $u_i \in \mathbb{H}^1(\Omega)$ satisfying $\|u_i\|_{\mathbb{H}^1(\Omega)} \leq M$ for $i = 1, 2$, their $\mathbb{L}^\infty(\Omega)$ norms are also bounded by some constant depending on M such that we could apply the local Lipschitz continuity of $g(x, u)$ in (2.3) to get

$$\int_{\Omega} |g(x, u_1) - g(x, u_2)|^2 dx \leq [C(M)]^2 \int_{\Omega} |u_1 - u_2|^2 dx = [C(M)]^2 \|u_1 - u_2\|_{\mathbb{L}^2(\Omega)}^2.$$

The two- and three-dimensional cases can be proved in a similar and simpler manner without relying on M based on the Assumption C, and we thus omit the details. \square

Now we introduce the control-to-state operator $G : \mathbb{H}^1(\Omega) \rightarrow Y := \mathbb{H}^2(\Omega) \cap \mathbb{H}_0^1(\Omega)$. We first show that G is well-defined.

THEOREM 2.2. *Under Assumptions A and B for one-dimensional case (or Assumptions A and C for two- and three-dimensional cases), the state equation (1.2) with $u \in \mathbb{H}^1(\Omega)$ has a unique solution $y = G(u) \in Y$, which is continuous on $\bar{\Omega}$ and satisfies*

$$\|y\|_{\mathbb{H}^2(\Omega)} \leq C(1 + \|u\|_{\mathbb{H}^1(\Omega)}^s), \quad 1 \leq s < \infty,$$

where C is independent of u .

Proof. By (2.1), $u \in \mathbb{H}^1(\Omega)$ implies $\mathcal{G}(u) \in \mathbb{L}^2(\Omega)$ and then we could follow the same approach as [5, Theorem 4] to prove that the state equation (1.2) has a unique solution $y \in Y$ that satisfies

$$\|y\|_{\mathbb{H}^2(\Omega)} \leq C \|1 + \mathcal{G}(u)\|_{\mathbb{L}^2(\Omega)} \leq C(1 + \|u\|_{\mathbb{H}^1(\Omega)}^s).$$

The continuity of y follows immediately from the Sobolev embedding theorem. \square

Next, we show that G is locally Lipschitz continuous with respect to u .

THEOREM 2.3. *Under Assumptions A and B for one-dimensional case (or Assumptions A and C for two- and three-dimensional cases), for any $M > 0$ there exists a constant $C(M) > 0$ such that the following relation holds for any $u_i \in \mathbb{H}^1(\Omega)$ with $\|u_i\|_{\mathbb{H}^1(\Omega)} \leq M$ for $i = 1, 2$*

$$(2.5) \quad \|G(u_1) - G(u_2)\|_{\mathbb{H}^2(\Omega)} \leq C(M) \|u_1 - u_2\|_{\mathbb{L}^2(\Omega)}.$$

Proof. For any $M > 0$, pick $u_1, u_2 \in \mathbb{H}^1(\Omega)$ such that $\|u_i\|_{\mathbb{H}^1(\Omega)} < M$ for $i = 1, 2$. By (2.2) there exist continuous states $y_i = G(u_i)$ for $i = 1, 2$. We then subtract the corresponding state equations to get

$$\begin{aligned} & \mathcal{A}(y_1 - y_2) + d(x, y_1) - d(x, y_2) \\ &= \mathcal{A}(y_1 - y_2) + \int_0^1 d_y(x, y_2 + \theta(y_1 - y_2)) d\theta \cdot (y_1 - y_2) \\ &=: \mathcal{A}(y_1 - y_2) + \phi(x)(y_1 - y_2) = \mathcal{G}(u_1) - \mathcal{G}(u_2). \end{aligned}$$

Thus, $y_1 - y_2$ satisfies a linear elliptic equation with zero boundary conditions. By Assumption A and (2.2), we have $\phi \in \mathbb{L}^\infty(\Omega)$. Furthermore, $d_y > 0$ in Assumption A implies $\phi(x) > 0$. Thus, the linear elliptic problem with respect to $y_1 - y_2$ has a unique weak solution in $\mathbb{H}^2(\Omega)$ with the regularity estimate [15, Chapter 6, Theorem 4]

$$\|y_1 - y_2\|_{\mathbb{H}^2(\Omega)} \leq C \|\mathcal{G}(u_1) - \mathcal{G}(u_2)\|_{\mathbb{L}^2(\Omega)} \leq C(M) \|u_1 - u_2\|_{\mathbb{L}^2(\Omega)}$$

where we have used the local Lipschitz continuity of \mathcal{G} in (2.4). \square

2.2. Existence of optimal control. We prove the existence of an optimal control for the problem (1.1)–(1.2) in the following theorem.

THEOREM 2.4. *Under Assumptions A and B for one-dimensional case (or Assumptions A and C for two- and three-dimensional cases), there exists an optimal control $\bar{u} \in \mathbb{H}^1(\Omega)$ for (1.1)–(1.2) satisfying $J(\bar{y}, \bar{u}) \leq J(y, u)$ for all $u \in \mathbb{H}^1(\Omega)$, where $\bar{y} = G(\bar{u})$ and $y = G(u)$.*

Proof. Since J is nonnegative and bounded below, there exists a minimizing sequence [24, Theorem 2.16]

$$\{u_j\}_{j \in \mathbb{N}} \subset U := \left\{ u \in \mathbb{H}^1(\Omega) \mid \|u\|_{\mathbb{H}^1(\Omega)} \leq B \right\}$$

for some $B > 0$ such that

$$J(G(u_j), u_j) \rightarrow m := \inf_{u \in \mathbb{H}^1(\Omega)} J(G(u), u) \text{ as } j \rightarrow \infty.$$

Then we aim to find a control \bar{u} (with $\bar{y} = G(\bar{u})$) to which the minimizing sequence converges such that $J(\bar{y}, \bar{u}) = m$.

Since $\{u_j\}_{j \in \mathbb{N}}$ is a bounded sequence in $U \subset \mathbb{H}^1(\Omega)$, there exists a weakly convergent subsequence $\{u_j\}_{j \in \mathcal{I}_1}$ with $\mathcal{I}_1 \subset \mathbb{N}$ such that

$$u_j \rightharpoonup \bar{u} \text{ in } \mathbb{H}^1(\Omega) \text{ as } j \rightarrow \infty \text{ in } \mathcal{I}_1 \text{ for some } \bar{u} \in \mathbb{H}^1(\Omega).$$

As $\mathbb{H}^1(\Omega)$ is compactly embedded into $\mathbb{L}^2(\Omega)$, we apply the Rellich–Kondrachov theorem [15, Chapter 5, Theorem 1] to get

$$u_j \rightarrow \bar{u} \text{ in } \mathbb{L}^2(\Omega) \text{ as } j \rightarrow \infty \text{ in } \mathcal{I}_1.$$

Since $\{u_j\}_{j \in \mathcal{I}_1} \subset U$ and $\bar{u} \in \mathbb{H}^1(\Omega)$, their \mathbb{H}^1 norms are bounded by some constant M such that we apply (2.4) to get

$$(2.6) \quad \|\mathcal{G}(u_j) - \mathcal{G}(\bar{u})\|_{\mathbb{L}^2(\Omega)} \leq C(M) \|u_j - \bar{u}\|_{\mathbb{L}^2(\Omega)} \rightarrow 0, \text{ as } j \rightarrow \infty \text{ in } \mathcal{I}_1$$

for some $C(M) > 0$, which implies that $\{\mathcal{G}(u_j)\}_{j \in \mathcal{I}_1}$ converges strongly in $\mathbb{L}^2(\Omega)$.

By (2.2) and $\|y_j\|_{\mathbb{H}^1(\Omega)} \leq M$ for $j \in \mathcal{I}_1$, $\{y_j\}_{j \in \mathcal{I}_1}$ and thus $\{d(x, y_j)\}_{j \in \mathcal{I}_1}$ (based on (2.1)) are uniformly bounded in $\mathbb{L}^\infty(\Omega)$ and hence in $\mathbb{L}^2(\Omega)$. Therefore, there exists an $\mathcal{I}_2 \subset \mathcal{I}_1$ such that $d(x, y_j) \rightarrow \bar{d}$ in $\mathbb{L}^2(\Omega)$ as $j \rightarrow \infty$ in \mathcal{I}_2 . Furthermore, (2.6) implies that $g(x, u_j) \rightarrow g(x, \bar{u})$ in $\mathbb{L}^2(\Omega)$ as $j \rightarrow \infty$ in \mathcal{I}_2 . Combine the above results to get $R_j := g(x, u_j) - d(x, y_j) \rightarrow R := g(x, \bar{u}) - \bar{d}$ in $\mathbb{L}^2(\Omega)$ as $j \rightarrow \infty$ in \mathcal{I}_2 , which, together with $y_j = \mathcal{A}^{-1}R_j$ and the fact that $\mathcal{A}^{-1} : \mathbb{L}^2(\Omega) \rightarrow Y$ is a continuous linear operator [15, Chapter 6, Theorem 1], leads to

$$(2.7) \quad y_j \rightarrow \bar{y} \text{ in } Y \text{ as } j \rightarrow \infty \text{ in } \mathcal{I}_2 \text{ for some } \bar{y} \in Y.$$

By the compact embedding $Y \hookrightarrow \mathbb{L}^2(\Omega)$, we have the strong convergence in $\mathbb{L}^2(\Omega)$

$$(2.8) \quad y_j \rightarrow \bar{y} \text{ in } \mathbb{L}^2(\Omega) \text{ as } j \rightarrow \infty \text{ in } \mathcal{I}_2.$$

Based on (2.2) in Assumption A, the Nemytskii operator $\mathcal{D} : y \rightarrow d(\cdot, y(\cdot))$ is locally Lipschitz continuous [24, Lemma 4.11], that is, for any $E > 0$ and y_1, y_2 satisfying $\|y_i\|_{\mathbb{L}^\infty(\Omega)} \leq E$ ($i = 1, 2$), there exists a constant $C(E) > 0$ such that

$$\|\mathcal{D}(y_1) - \mathcal{D}(y_2)\|_{\mathbb{L}^2(\Omega)} \leq C(E) \|y_1 - y_2\|_{\mathbb{L}^2(\Omega)}.$$

From (2.2), the sequence $\{y_j\}_{j \in \mathcal{I}_2}$ and its limit \bar{y} are uniformly bounded under the $\mathbb{L}^\infty(\Omega)$ norm such that we invoke (2.8) to get

$$(2.9) \quad \|\mathcal{D}(y_j) - \mathcal{D}(\bar{y})\|_{\mathbb{L}^2(\Omega)} \leq C \|y_j - \bar{y}\|_{\mathbb{L}^2(\Omega)} \rightarrow 0 \text{ as } j \rightarrow \infty \text{ in } \mathcal{I}_2.$$

We then calculate the inner product of the state equation $\mathcal{A}y_j + d(x, y_j) = g(x, u_j)$ ($j \in \mathcal{I}_2$) and $\phi \in Y$ to get

$$\int_{\Omega} a(x) \nabla y_j \nabla \phi + c(x) y_j \phi \, dx + \int_{\Omega} d(x, y_j) \phi \, dx = \int_{\Omega} g(x, u_j) \phi \, dx.$$

Combine this with various convergence results, i.e. (2.6)–(2.7) and (2.9), to obtain

$$\int_{\Omega} a(x) \nabla \bar{y} \nabla \phi + c(x) \bar{y} \phi \, dx + \int_{\Omega} d(x, \bar{y}) \phi \, dx = \int_{\Omega} g(x, \bar{u}) \phi \, dx.$$

Since ϕ is arbitrarily chosen in Y , we have $\bar{y} = G(\bar{u})$.

With the assistance of the above results, we turn to prove the main result. Let $J(y, u) = \Phi(y) + \Psi(u)$ where $\Phi(y) := \frac{1}{2} \|y - y_d\|_{\mathbb{L}^2(\Omega)}^2$ and $\Psi(u) := \frac{\lambda}{2} \|u\|_{\mathbb{H}^1(\Omega)}^2$.

Since the \mathbb{H}^1 norms of $\{u_j\}_{j \in \mathcal{I}_1}$ and \bar{u} are bounded by some constant M (as mentioned above (2.6)) and $\{u_j\}_{j \in \mathcal{I}_1}$ converges strongly to \bar{u} in $\mathbb{L}^2(\Omega)$, (2.5) implies that $G(u_j) \rightarrow G(\bar{u}) = \bar{y}$ in $\mathbb{L}^2(\Omega)$ as $j \rightarrow \infty$ in \mathcal{I}_1 such that

$$\lim_{j \rightarrow \infty} \Phi(G(u_j)) = \Phi(G(\bar{u})) = \Phi(\bar{y}) \text{ as } j \rightarrow \infty \text{ in } \mathcal{I}_1.$$

Furthermore, as $\{u_j\}_{j \in \mathcal{I}_1}$ is a weakly convergent sequence to \bar{u} in $\mathbb{H}^1(\Omega)$, the convexity and weak lower semicontinuity of Ψ imply

$$\Psi(\bar{u}) \leq \liminf_{j \rightarrow \infty} \Psi(u_j).$$

Combine the above two estimates to get for $j \in \mathcal{I}_1$

$$m = \lim_{j \rightarrow \infty} J(G(u_j), u_j) = \lim_{j \rightarrow \infty} \Phi(G(u_j)) + \liminf_{j \rightarrow \infty} \Psi(u_j) \Phi(\bar{y}) + \Psi(\bar{u}) = J(\bar{y}, \bar{u}),$$

which, together with $m \leq J(\bar{y}, \bar{u})$, implies the existence of an optimal control \bar{u} with the associated state $\bar{y} = G(\bar{u})$. \square

3. Constructing control landscape. We propose the algorithm of constructing control landscape by PCHiSD to solve the non-convex optimal control from a comprehensive and global perspective. Both the unconstrained optimal control (1.1)–(1.2) and the case with an integral constraint will be considered.

3.1. Review of HiSD. For $w, v \in \mathbb{R}^m$, we denote the inner product and the norm as $\langle w, v \rangle = w^\top v$ and $\|w\| = \sqrt{\langle w, w \rangle}$, respectively. Let $E(w)$ be an energy functional which is at least twice differentiable with respect to $w \in \mathbb{R}^m$, and denote its gradient and Hessian as $\nabla E(w)$ and $H(w) := \nabla^2 E(w)$, respectively. Then the HiSD for searching an index- k saddle point reads [29]

$$(3.1) \quad \begin{cases} \dot{w} = -\beta \left(I - 2 \sum_{j=1}^k v_j v_j^\top \right) \nabla E(w), \\ \dot{v}_i = -\gamma \left(I - v_i v_i^\top - 2 \sum_{j=1}^{i-1} v_j v_j^\top \right) H(w) v_i, \quad i = 1, \dots, k. \end{cases}$$

Here $w \in \mathbb{R}^m$ is the state variable, $\{v_i\}_{i=1}^k \subset \mathbb{R}^m$ are directional variables that support the evolution of the dynamics of w , and β and γ are relaxation parameters. The dynamics of w is a combination of an upward search in the unstable subspace of the target saddle point and a downward search in its stable subspace, while the dynamics of directional variables is derived from minimizing the Rayleigh quotient subject to the orthonormality constraint. It is proved in [29] that a linearly stable stationary point of HiSD is an index- k saddle point, which theoretically substantiates the effectiveness of HiSD in locating saddle points. Furthermore, the orthonormality of the initial conditions $\{v_{i,0}\}_{i=1}^k$ implies that of $\{v_i\}_{i=1}^k$ for any $t > 0$.

In practice, explicitly computing and storing the Hessian may be expensive and time-consuming, and we usually adopt the dimer method to approximate the product of the Hessian and a vector. Specifically, given a dimer length $l > 0$ and a vector v , the $H(w)v$ could be approximated by $\tilde{H}(w, v, l)$ via the center difference scheme

$$H(w)v \approx \tilde{H}(w, v, l) := \frac{\nabla E(w + lv) - \nabla E(w - lv)}{2l}.$$

For practical computation, we discretize HiSD by the explicit Euler scheme, where the position variable w evolves as

$$(3.2) \quad w^{(n+1)} = w^{(n)} - \beta_n \left(I - 2 \sum_{j=1}^k v_j^{(n)} v_j^{(n)\top} \right) \nabla E(w^{(n)}),$$

and the directional variables are updated as

$$(3.3) \quad \begin{aligned} \hat{v}_i^{(n+1)} &= v_i^{(n)} - \gamma_n \tilde{H}(w^{(n)}, v_i^{(n)}, l), \quad i = 1, \dots, k, \\ \{v_i^{(n+1)}\}_{i=1}^k &= \text{Orth} \{\hat{v}_i^{(n+1)}\}_{i=1}^k. \end{aligned}$$

Here β_n and γ_n serve as time-step sizes and the operator “Orth” refers to the standard Gram–Schmidt orthonormalization process. It is worth mentioning that although the schemes of directional variables in (3.3) look different from their continuous formulations in (3.1), they are inherently consistent, as proved in [30]. Furthermore, we employ the Barzilai–Borwein (BB) method to perform an adaptive step-size selection [3, 29].

3.2. PCHiSD for optimal control. By the control-to-state operator G , the cost functional J could be rewritten as a reduced cost functional $\hat{J}(u) := J(y, u) = J(G(u), u)$. We then prove its differentiability and derive its gradient operator by means of first-order variational analysis.

THEOREM 3.1. *Under Assumptions A and B for one-dimensional case (or Assumptions A and C for two- and three-dimensional cases), \hat{J} is Fréchet differentiable and its gradient operator is given as*

$$\hat{J}'(u) = \lambda(-\Delta u + u) + pg_u(x, u), \quad u \in \mathbb{H}^1(\Omega),$$

where $p \in Y$ denotes the adjoint variable uniquely determined by the adjoint equation associated with the corresponding state $y = G(u)$

$$(3.4) \quad \begin{cases} \mathcal{A}p + d_y(x, y)p = y - y_d & \text{in } \Omega, \\ p = 0 & \text{on } \Gamma. \end{cases}$$

Proof. Define $A : Y \times \mathbb{H}^1(\Omega) \rightarrow \mathbb{L}^2(\Omega)$ as

$$A(y, u) := \mathcal{A}y + d(x, y) - g(x, u).$$

Since d and g are continuously differentiable with respect to y and u , respectively, we have $A \in C^1(Y \times \mathbb{H}^1(\Omega), \mathbb{L}^2(\Omega))$. Let $\delta u \in \mathbb{H}^1(\Omega)$ and $(y, u) \in Y \times \mathbb{H}^1(\Omega)$ with $y = G(u)$. The directional derivative of $A(G(u), u)$ at u along δu satisfies

$$A'(G(u), u)\delta u = A_y(G(u), u)G'(u)\delta u - A_u(G(u), u)\delta u = 0,$$

which, together with $\delta y = G'(u)\delta u$ and (1.2), leads to

$$(3.5) \quad A'(G(u), u)\delta u = \mathcal{A}\delta y + d_y(x, y)\delta y - g_u(x, u)\delta u = 0.$$

According to Assumption A, we have $d_y(x, y_0) \in \mathbb{L}^\infty(\Omega)$ and $d_y(x, y) > 0$ such that the Lax–Milgram theorem [15, Chapter 5, Theorem 1] implies that $A_y(y_0, u_0) : \mathbb{H}_0^1(\Omega) \rightarrow \mathbb{H}^{-1}(\Omega)$ is a bounded bijection. Hence $A_y^{-1}(y_0, u_0) \in \mathcal{L}(\mathbb{H}^{-1}(\Omega), \mathbb{H}_0^1(\Omega))$. By the implicit function theorem, there exists a unique mapping G , i.e., the control-to-state operator, satisfying $A(G(u_0), y_0) = 0$. Moreover, since $A(y_0, u_0)$ is C^1 , we have $G \in C^1(\mathbb{H}^1(\Omega), Y)$, and thus $\hat{J}(u)$ is differentiable.

Then for $u, \delta u \in \mathbb{H}^1(\Omega)$, we invoke (3.4) and (3.5) to obtain

$$\begin{aligned}
\hat{J}'(u)\delta u &= \frac{d}{dt} \hat{J}(u + t\delta u)|_{t=0} \\
&= \int_{\Omega} (y - y_d)G'(u)\delta u dx + \lambda \int_{\Omega} (-\Delta u + u)\delta u dx \\
&= \int_{\Omega} (\mathcal{A}p + d_y(x, y)p)\delta y dx + \lambda \int_{\Omega} (-\Delta u + u)\delta u dx \\
&= \int_{\Omega} (\mathcal{A}\delta y + d_y(x, y)\delta y)p dx + \lambda \int_{\Omega} (-\Delta u + u)\delta u dx \\
&= \int_{\Omega} [g_u(x, u)p + \lambda(-\Delta u + u)]\delta u dx.
\end{aligned}$$

Thus we complete the proof. \square

Based on Theorem 3.1, any stationary point u (i.e. either a saddle point or a minimum) of optimal control (1.1)–(1.2) satisfies $\hat{J}'(u) = 0$ on Ω with $u = 0$ on Γ . Thus, we aim to design the PCHiSD for computing multiple solutions of $\hat{J}'(u) = 0$.

To present the algorithm, we need to first perform spatial discretization for $\hat{J}'(u)$ and then use this to replace ∇E in the HiSD algorithm (3.2)–(3.3) for possible computation. For demonstration, we consider a two-dimensional rectangular domain $\Omega := [0, 1]^2$ and perform the finite difference discretization for encountered spatial differential operators. Nevertheless, it is worth mentioning that more general domains and other spatial discretization methods could be adopted if we first recover the HiSD to its continuous-in-space formulation, invoke the expression of $\hat{J}'(u)$ in this formulation to get an evolutionary parabolic system and then apply appropriate spatial and temporal discretizations, see [31, 32] for preliminary investigations of this idea.

For $\Omega := [0, 1]^2$, define a uniform grid for some $0 < N \in \mathbb{N}$

$$\Omega_h := \{(X_{1,i}, X_{2,j}) \mid i, j = 1, \dots, N-1\}, \quad X_{1,i} = ih, \quad X_{2,j} = jh, \quad h = \frac{1}{N}.$$

Then we discretize $\hat{J}'(u)$ as

$$(3.6) \quad \hat{J}'_h(u_h) = \lambda(L + I)u_h + p_h \odot g_{u,h}(u_h),$$

where $u_h = [u_{1,1}, \dots, u_{N-1,N-1}]^\top \in \mathbb{R}^m$ with $m := (N-1)^2$, L is the stiffness matrix derived from the finite difference discretization of \mathcal{A} under zero Dirichlet boundary conditions, I is the identity matrix, $g_{u,h}(u_h) := [g_{u,1,1}, \dots, g_{u,N-1,N-1}]^\top$ with $g_{u,i,j} = g_u([X_{1,i}, X_{2,j}], u_{i,j})$, and $p_h = [p_{1,1}, \dots, p_{N-1,N-1}]^\top$. The symbol \odot denotes the Hadamard (elementwise) product of two vectors.

Note that in (3.6), the p_h is not directly given, which is the critical difference from usual multiple solution computations of energy functionals by HiSD. Indeed, for a given discrete control variable u_h , one need to first determine the discrete state variable y_h by solving the discrete state equation

$$(3.7) \quad Ly_h + d_h(y_h) - g_h(u_h) = 0.$$

where $d_h(y_h) := [d_{1,1}, \dots, d_{N-1,N-1}]^\top$ and $g_h(u_h) := [g_{1,1}, \dots, g_{N-1,N-1}]^\top$ with $d_{i,j} = d([X_{1,i}, X_{2,j}], y_{i,j})$ and $g_{i,j} = g([X_{1,i}, X_{2,j}], u_{i,j})$, and then determine the discrete

adjoint variable p_h by solving the discrete adjoint equation

$$(3.8) \quad [L + Id_{y,h}(y_h)]^\top p_h = y_h - y_{d,h},$$

where $d_{y,h}(y_h) := [d_{y,1,1}, \dots, d_{y,N-1,N-1}]^\top$ and $y_{d,h} = [y_{d,1,1}, \dots, y_{d,N-1,N-1}]^\top$ with $d_{y,i,j} = d_y([X_{1,i}, X_{2,j}], y_{i,j})$ and $y_{d,i,j} = y_d([X_{1,i}, X_{2,j}], y_{i,j})$.

In summary, with the assistance of intermediate computations (3.7)–(3.8) for evaluating \hat{J}'_h , we can replace $-\nabla E$ by \hat{J}'_h in (3.2)–(3.3) to get the following PCHiSD for numerically searching an index- k saddle point of the reduced cost functional \hat{J}

$$\left\{ \begin{array}{l} \text{Auxiliary} \\ \text{PDE solvers} \\ \text{HiSD scheme} \end{array} \right\} \begin{cases} Ly_{h,i}^{(n,\pm)} + d_h(y_{h,i}^{(n,\pm)}) - g_h(u_{h,i}^{(n,\pm)}) = 0, \\ [L + Id_{y,h}(y_{h,i}^{(n,\pm)})]^\top p_{h,i}^{(n,\pm)} = y_{h,i}^{(n,\pm)} - y_{d,h}, \\ u_h^{(n+1)} = u_h^{(n)} + \beta_n \left(I - 2 \sum_{j=1}^k v_j^{(n)} v_j^{(n)\top} \right) \hat{J}'_h(u_h^{(n)}), \\ \hat{v}_{h,i}^{(n+1)} = v_{h,i}^{(n)} + \gamma_n \tilde{H}(u_h^{(n)}, v_{h,i}^{(n)}, l), \\ \{v_{h,i}^{(n+1)}\}_{i=1}^k = \text{Orth} \{ \hat{v}_{h,i}^{(n+1)} \}_{i=1}^k, \end{cases} \quad i = 0, 1, \dots, k,$$

equipped with the initial conditions $u_h^{(0)}$ and $\{v_{h,i}^{(0)}\}_{i=1}^k$ satisfying $(v_{h,j}^{(0)})^\top v_{h,i}^{(0)} = \delta_{ij}$ for $1 \leq i, j \leq k$. Here $y_{h,i}^{(n,\pm)}$ and $p_{h,i}^{(n,\pm)}$ denote the state and adjoint variables associated with the controls $u_{h,i}^{(n,\pm)}$ defined as

$$\begin{cases} u_{h,0}^{(n,\pm)} = u_h^{(n)}, \\ u_{h,i}^{(n,+)} = u_h^{(n)} + lv_{h,i}^{(n)}, \quad i = 1, \dots, k, \\ u_{h,i}^{(n,-)} = u_h^{(n)} - lv_{h,i}^{(n)}, \quad i = 1, \dots, k, \end{cases}$$

and

$$(3.9) \quad \tilde{H}(u_h^{(n)}, v_{h,i}^{(n)}, l) := \frac{J'_h(u_{h,i}^{(n,+)}) - J'_h(u_{h,i}^{(n,-)})}{2l}, \quad i = 1, \dots, k.$$

For clarity, we summarize the PCHiSD algorithm for searching an index- k saddle point of the reduced cost functional \hat{J} (and thus the optimal control (1.1)–(1.2)) as follows.

3.3. Construction of control landscape. With the assistance of the PCHiSD in locating saddle points of the optimal control (1.1)–(1.2), we explain how to construct its control landscape. Following [28], the downward and upward search algorithms will be adopted, where the former starts from a high-index saddle point to locate saddle points of lower indices and the latter ascends from a low-index point toward saddle points of higher indices. By combining these two search methods, we could systematically locate multiple saddle points of the optimal control (1.1)–(1.2) to generate its control landscape.

We present details for the downward search, which is frequently used in constructing the control landscape from a parent state, as we will do in numerical experiments (more details on downward and upward searches can be found in [28]). Suppose that $u^{(k)}$ represents an index- k saddle point with eigenvectors (stored column-wise in $V^{(k)} := [v_1, v_2, \dots, v_k]$) constituting unstable subspaces. To search for an index- r

Algorithm 3.1 PCHiSD for optimal control (1.1)–(1.2)

Input: $k \in \mathbb{N}$, $\beta_0, \gamma_0, l, \epsilon > 0$, $u_h^{(0)}, \{v_{h,i}^{(0)}\}_{i=1}^k$ with $(v_{h,j}^{(0)})^\top v_{h,i}^{(0)} = \delta_{ij}$.
 Set $n = 0$ and $V^{(0)} = [v_{h,1}^{(0)}, \dots, v_{h,k}^{(0)}]$;
repeat
 Calculate $y_h^{(n)}$ and $p_h^{(n)}$ from (3.7) and (3.8) by Newton's method;
 Calculate $J_h^{(n)} := J_h'(u_h^{(n)})$ by (3.6);
 Select time-step sizes β_n and γ_n ;
 $u_h^{(n+1)} = u_h^{(n)} + \beta_n(I - 2V^{(n)}V^{(n)\top})J_h^{(n)}$;
 for $i = 1 : k$ **do**
 Calculate $y_{h,i}^{(n,\pm)}$ and $p_{h,i}^{(n,\pm)}$ from (3.7) and (3.8) by Newton's method;
 Calculate $\tilde{H}_i^{(n)} := \tilde{H}(u_h^{(n)}, v_{h,i}^{(n)}, l)$ by (3.9);
 $v_i^{(n+1)} = v_{h,i}^{(n)} + \gamma_n \tilde{H}_i^{(n)}$;
 end for
 $V^{(n+1)} = \text{Orth}[v_{h,1}^{(n+1)}, \dots, v_{h,k}^{(n+1)}]$;
 $n = n + 1$;
until $\|J_h^{(n+1)}\| < \epsilon$
Output: An index- k saddle point $u^{(n+1)}$.

saddle point ($r < k$) from $u^{(k)}$, we first select one direction v_i with $1 \leq i \leq r$ from $V^{(k)}$ and perturb $u^{(k)}$ along v_i to obtain the initial state of control variable $u^{(r)}$, that is, $u^{(r)} = u^{(k)} \pm \sigma v_i$ for some $\sigma > 0$. Then we choose r unstable directions from the remaining set $V^{(k)} \setminus \{v_i\}$ to get the initial directions $V^{(r)} := \{\tilde{v}_1, \tilde{v}_2, \dots, \tilde{v}_r\}$. With these initial conditions, we can apply Algorithm 3.1 to locate an index- r saddle point.

3.4. Extension to integral constraint case. We extend the study to optimal control (1.1)–(1.2) with an integral constraint $\int_\Omega u(x)dx = c$ for some $c \in \mathbb{R}$, that is, we consider

$$(3.10) \quad \min_{u \in U_{ad}} \hat{J}(u) = \frac{1}{2} \|G(u) - y_d\|_{L^2(\Omega)}^2 + \frac{\lambda}{2} \|u\|_{\mathbb{H}^1(\Omega)}^2,$$

where

$$(3.11) \quad U_{ad} := \{u \in \mathbb{H}^1(\Omega) \mid \int_\Omega u(x)dx = c\}.$$

For constrained problems, the standard approach is to incorporate the constraints into the first-order optimality condition. However, the saddle dynamics algorithm provides a new perspective by embedding the constraint into the dynamical system [27], where the core idea is to restrict the problem to a Riemannian manifold that incorporates the constraint and then perform unconstrained optimization on the manifold.

To present the details of implementation, let $\mathcal{C}(u_h) := \frac{1}{m} \mathbf{1}^\top u_h - c = 0$ be the discrete integral constraint where $\mathbf{1} = (1, 1, \dots, 1)^\top \in \mathbb{R}^m$, and let $\nabla \mathcal{C}(u_h)$ denote the gradient of the constraint. Then the corresponding orthogonal normal space and tangent space at u_h are defined respectively as $N(u_h) = \text{span}\{\nabla \mathcal{C}(u_h)\}$ and $T(u_h) = \{v \in \mathbb{R}^m \mid \nabla \mathcal{C}(u_h)^\top v = 0\}$. The orthogonal projection onto the tangent space is given by

$$\mathcal{P}_T = I - \frac{\nabla \mathcal{C}(u_h) \nabla \mathcal{C}(u_h)^\top}{\|\nabla \mathcal{C}(u_h)\|^2} = I - \frac{1}{m} \mathbf{1} \mathbf{1}^\top.$$

Consequently, the constrained optimal control problem can be reformulated as an unconstrained optimization problem on the Riemannian manifold $\mathcal{M} = \{u_h \in \mathbb{R}^m \mid \mathcal{C}(u_h) = 0\}$. On this manifold, we define the Riemannian gradient $\mathcal{P}_T \hat{J}'_h(u_h)$ such that the PCHiSD for computing saddle points of the constrained optimal control (3.10)–(3.11) reads

$$(3.12) \quad \left\{ \begin{array}{l} \text{Auxiliary} \\ \text{PDE solvers} \end{array} \right\} \begin{cases} Ly_{h,i}^{(n,\pm)} + d_h(y_{h,i}^{(n,\pm)}) - g_h(u_{h,i}^{(n,\pm)}) = 0, \\ [L + Id_{y,h}(y_{h,i}^{(n,\pm)})]^\top p_{h,i}^{(n,\pm)} = y_{h,i}^{(n,\pm)} - y_{d,h}, \end{cases} \quad i = 0, 1, \dots, k, \\ \left\{ \begin{array}{l} \text{HiSD scheme} \end{array} \right\} \begin{cases} u_h^{(n+1)} = u_h^{(n)} + \beta_n \left(I - 2 \sum_{j=1}^k v_j^{(n)} v_j^{(n)\top} \right) \mathcal{P}_T \hat{J}'_h(u_h^{(n)}), \\ \hat{v}_{h,i}^{(n+1)} = v_{h,i}^{(n)} + \gamma_n \mathcal{P}_T \tilde{H}(u_h^{(n)}, v_{h,i}^{(n)}, l), \\ \{v_{h,i}^{(n+1)}\}_{i=1}^k = \text{Orth} \{ \hat{v}_{h,i}^{(n+1)} \}_{i=1}^k, \end{cases} \quad i = 1, \dots, k,$$

equipped with the initial conditions $u_h^{(0)}$ and $\{v_{h,i}^{(0)}\}_{i=1}^k$ satisfying $\int_\Omega u_h^{(0)}(x)dx = c$ and $(v_{h,j}^{(0)})^\top v_{h,i}^{(0)} = \delta_{ij}$ for $1 \leq i, j \leq k$.

With the help of (3.12), one could follow the search methods in Section 3.3 to construct the control landscape of the constrained problem (3.10)–(3.11).

4. Numerical experiments. We present several numerical experiments and comparisons with classical methods to demonstrate the advantages of the control landscape method. When the index of the parent state is high and there are many intermediate saddle points, we omit most of them and focus on low-index ones in the control landscape.

4.1. Numerical comparison for one-dimensional problem. Let $\Omega = [0, 1]$, $a_{11}(x) = c(x) \equiv 1$, $d(x, y) = y^3$, $g(x, u) = 0.001u^2 + \cos(2\pi u)$ and $y_d = -2\sin(\pi x)$. A uniform partition is adopted with $h = 2^{-8}$.

Constructing control landscapes For different λ , the control landscapes of (1.1)–(1.2) are presented in Fig. 1, and each control landscape starts from a trivial state $u \equiv 0$ to perform a downward search for lower-index saddle points. When $\lambda = 0.02$, the control landscape of $\hat{J}(u)$ and the corresponding state landscape are shown, where $u \equiv 0$ is an index-4 saddle point and two minima can be located along the transition pathway, which correspond to the lowest value of $\hat{J}(u)$ such that they are most likely global minima (i.e. the optimal control). Furthermore, as the index of the control variable decreases, the corresponding state variable gets close to the target state y_d , as shown in the state landscape. These observations indicate that the control and state landscapes depict comprehensive patterns of control and state spaces of the optimal control, respectively, by means of stationary points, which provide rich information of optimal control and naturally locate its minima.

For the case $\lambda = 0.005$, six minima are found, two of which correspond to the lowest value of $\hat{J}(u)$ such that they are most likely global minima. When $\lambda = 0.0005$, the stronger non-convexity results in a much richer control landscape with many minima. Nevertheless, the control landscape could still locate them. Note that the control landscape method does not depend on the initial guess of u due to the employment of the information of high-index saddle points, which demonstrates its effectiveness and superiority.

Another observation from Fig. 1 is that a decrement of λ leads to a decrement of the lowest value of \hat{J} . A possible reason is that a decrement of λ implies that the

term $\|u\|_{\mathbb{H}^1(\Omega)}^2$ plays a less dominate role in \hat{J} such that the change of optimal control u is admitted to be more rapid, cf. Fig. 1, leading to a better approximation y to y_d and thus a smaller value of \hat{J} .

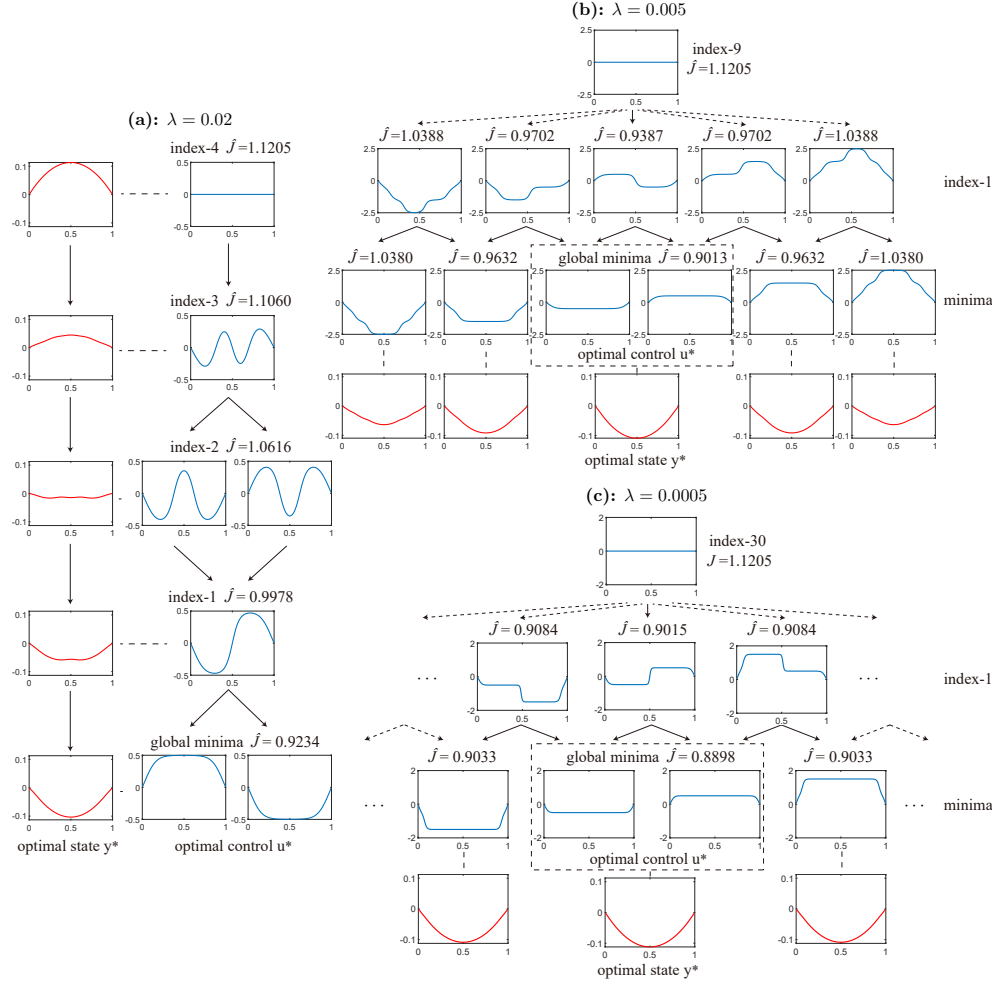


Fig. 1: Control landscapes of one-dimensional problem with different λ . Each plot shows either a distribution of the control u (blue curve) corresponding to a saddle point of the reduced cost functional \hat{J} , or the corresponding state y (red curve). The optimal control and the corresponding optimal state are denoted as u^* and y^* , respectively.

Comparison with Gradient and Newton's methods For comparison with the control landscape method, we test the performance of the BB gradient method [3] and Newton's method in solving optimal control (1.1)–(1.2). In the BB gradient method, we alternately use the BB1 and BB2 step sizes, which are respectively defined

by

$$\beta_{\text{BB1}}^{(n)} = \frac{\langle \Delta u_h^{(n)}, \Delta u_h^{(n)} \rangle}{\langle \Delta u_h^{(n)}, \Delta \hat{J}'_h(u_h^{(n)}) \rangle}, \quad \beta_{\text{BB2}}^{(n)} = \frac{\langle \Delta u_h^{(n)}, \Delta \hat{J}'_h(u_h^{(n)}) \rangle}{\langle \Delta \hat{J}'_h(u_h^{(n)}), \Delta \hat{J}'_h(u_h^{(n)}) \rangle}$$

with $\Delta u_h^{(n)} = u_h^{(n)} - u_h^{(n-1)}$ and $\Delta \hat{J}'_h(u_h^{(n)}) = \hat{J}'_h(u_h^{(n)}) - \hat{J}'_h(u_h^{(n-1)})$, to perform gradient descent for $\hat{J}(u)$. For application of the Newton's method, let $\mathcal{L}(y, p, u)$ denotes the Lagrangian function of the cost functional J subject to the state equation constraint, i.e.

$$\mathcal{L}(y, p, u) = J(y, u) + \int_{\Omega} p(\mathcal{A}y + d(x, y) - g(x, u))dx.$$

Then the Newton's method solves the following nonlinear system $\mathcal{L}'(y, p, u) = 0$ where the vector $\mathcal{L}'(y, p, u) := (\mathcal{L}_y(y, p, u), \mathcal{L}_p(y, p, u), \mathcal{L}_u(y, p, u))$ contains Fréchet derivatives of the Lagrangian function \mathcal{L} with respect to its variables. After spatial discretization, the main iterative procedure of the method is given by [5, 18]

$$\mathcal{H}^{(n)} \begin{bmatrix} \Delta y_h^{(n+1)}, \Delta p_h^{(n+1)}, \Delta u_h^{(n+1)} \end{bmatrix}^{\top} = -\mathcal{F}^{(n)},$$

where $\Delta y_h^{(n+1)} := y_h^{(n+1)} - y_h^{(n)}$, Δp_h and Δu_h are defined similarly, and

$$\mathcal{H}^{(n)} = \begin{bmatrix} L + I + \text{diag}(d_{y,h}(y_h^{(n)})) & O & -\text{diag}(g_h(u_h^{(n)})) \\ \text{diag}(d_{yy,h}(y_h^{(n)})) - I & L + I + \text{diag}(d_{y,h}(y_h^{(n)})) & O \\ O & \text{diag}(g_h(u_h^{(n)})) & \text{diag}(p_h^{(n)} \odot g_{uu,h}(u_h^{(n)})) \end{bmatrix},$$

$$\mathcal{F}^{(n)} = \begin{bmatrix} (L + I)y_h^{(n)} + d_h(y_h^{(n)}) - g_h(u_h^{(n)}) \\ (L + I)p_h^{(n)} + d_{y,h}(y_h^{(n)}) \odot p_h^{(n)} - y_h^{(n)} + y_{d,h} \\ -\lambda(L + I)u_h^{(n)} + g_h(u_h^{(n)}) \end{bmatrix},$$

where $\text{diag}(\cdot)$ denotes the operation that transforms a vector into a diagonal matrix.

In both iterative methods, different constant initial values of the control variable u are attempted over $[-10, 10]$, that is, we test the initial value of u as $-10 + 0.01j$ for $j = 0, 1, \dots, 2000$ in order, and the domains of convergence and the corresponding minima are presented in Fig. 2. We find that the convergence of both methods depend on the initial guesses of u , and in particular the algorithms could converge to global minima when the initial guesses are chosen from some narrow domains. As λ decreases, the domains of convergence also shrink, which increases the difficulty of locating minima. These observations indicate that the effectiveness of locating minima by both methods rely on appropriate initial guesses.

4.2. Control landscape for two-dimensional problems. We consider examples on $\Omega = [0, 1]^2$ with $a_{11}(x) = c(x) \equiv 1$, $d(x, y) = 0$ and $y_d = 2$. A uniform partition is adopted with $h = 2^{-5}$, and different cases are considered:

Case 1 (symmetric, unconstrained): $g(x, u) = e^{-(u+1)^2} + e^{-(u-1)^2} - e^{-u^2}$;

Case 2 (asymmetric, unconstrained): $g(x, u) = e^{-(u+1)^2} + e^{-(u-1)^2} - (1 + 0.8u^3)e^{-u^2}$;

Case 3 (asymmetric, constrained): $g(x, u) = e^{-(u+1)^2} + e^{-(u-1)^2} - (1 + 0.8u^3)e^{-u^2}$ with integral constraint $\int_{\Omega} u dx = 0$.

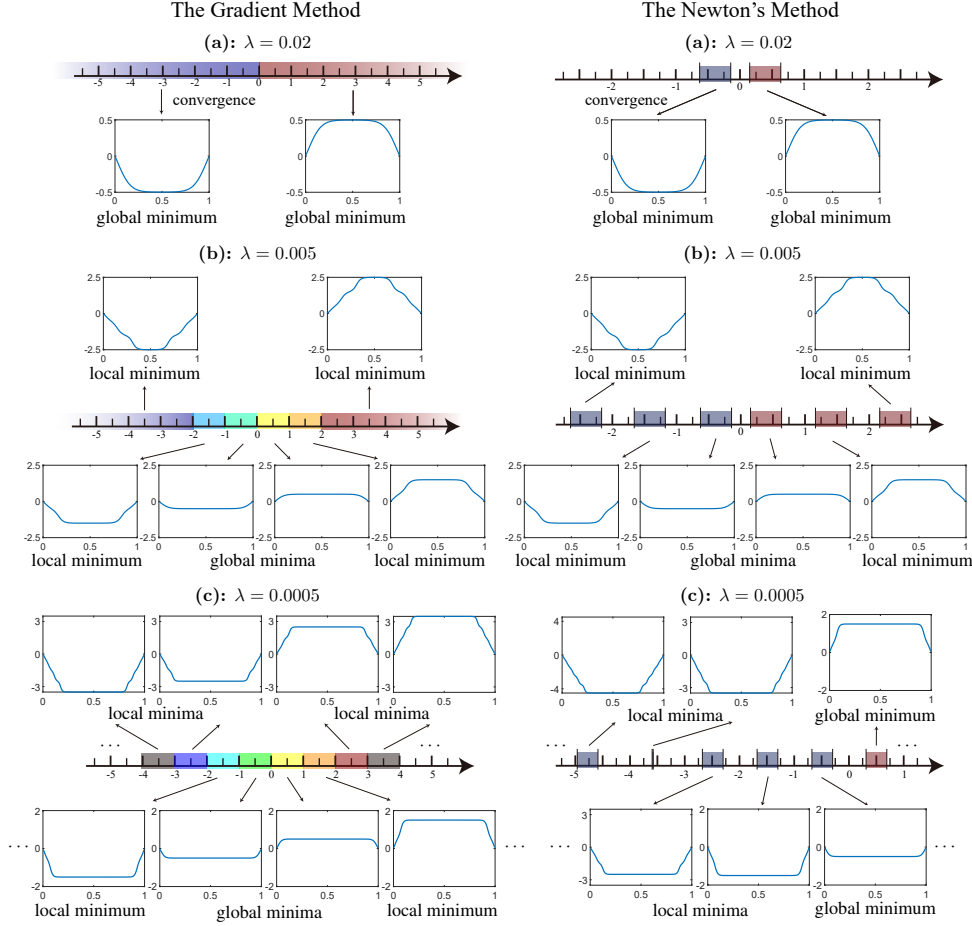


Fig. 2: Domains of convergence of the gradient method and the Newton's method. Each colored segment represents an interval in which the constant initial value of u could be selected such that the algorithm converges to the corresponding minima.

In Fig. 3, we present control and state landscapes of $\hat{J}(u)$ for Case 1. Similar to the one-dimensional case, a decrement of λ leads to a more complex pattern, and during the evolution of the control variable along the transition pathways in control landscape, the state variable gradually evolves toward the desired state and eventually reaches a stable optimal configuration. These numerical results again indicate the effectiveness of the control landscape in depicting comprehensive patterns of the non-convex optimal control and locating minima.

In Fig. 4, we consider the Case 2. Due to the broken symmetry, many deformations arise compared to the results in Fig. 3. For instance, two local optimal controls are obtained for each case of λ , but only one of them attains the lowest value of \hat{J} . Another interesting and unintuitive phenomenon is that some high-index saddle points correspond to smaller values of \hat{J} than those of the subsequent lower-index saddle points. For instance, in Fig. 4 (d), an index-3 saddle point corresponds to $\hat{J} = 1.8830$, while an index-2 saddle point corresponds to $\hat{J} = 1.8857$. We thus reach

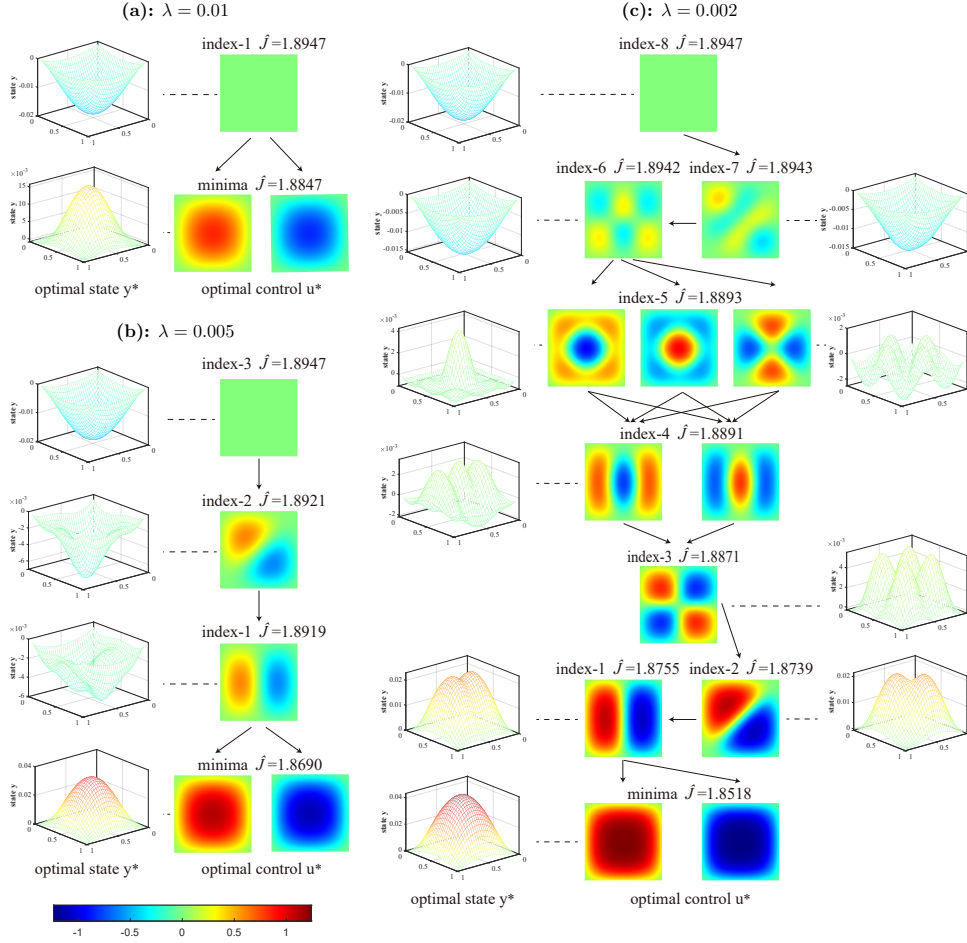


Fig. 3: Control landscapes of symmetric and unconstrained case 1 with $\lambda = 0.01, 0.005, 0.002$. Each colored plot shows the distribution of the control u , and each three-dimensional surface depicts the corresponding state y .

the following conclusions or comments:

- A lower-index saddle point may not necessarily be more optimal than a higher-index one. Moreover, asymmetric structures could further increase the non-convexity of the model and then break the energy-decreasing behavior along a transition pathway. Such phenomena are rarely encountered in other multiple solution problems and imply the necessity of computing multiple solutions of non-convex optimal control in order to find the optimal control.
- In practical applications, the feasibility of implementing the optimal control should be considered. If the optimal control is difficult to be realized in practice, one could still select other stationary points from the control landscape to balance the feasibility of the control and its optimality in terms of the value of \hat{J} .

Finally, we consider the Case 3 in Fig. 5, which shows that under the integral

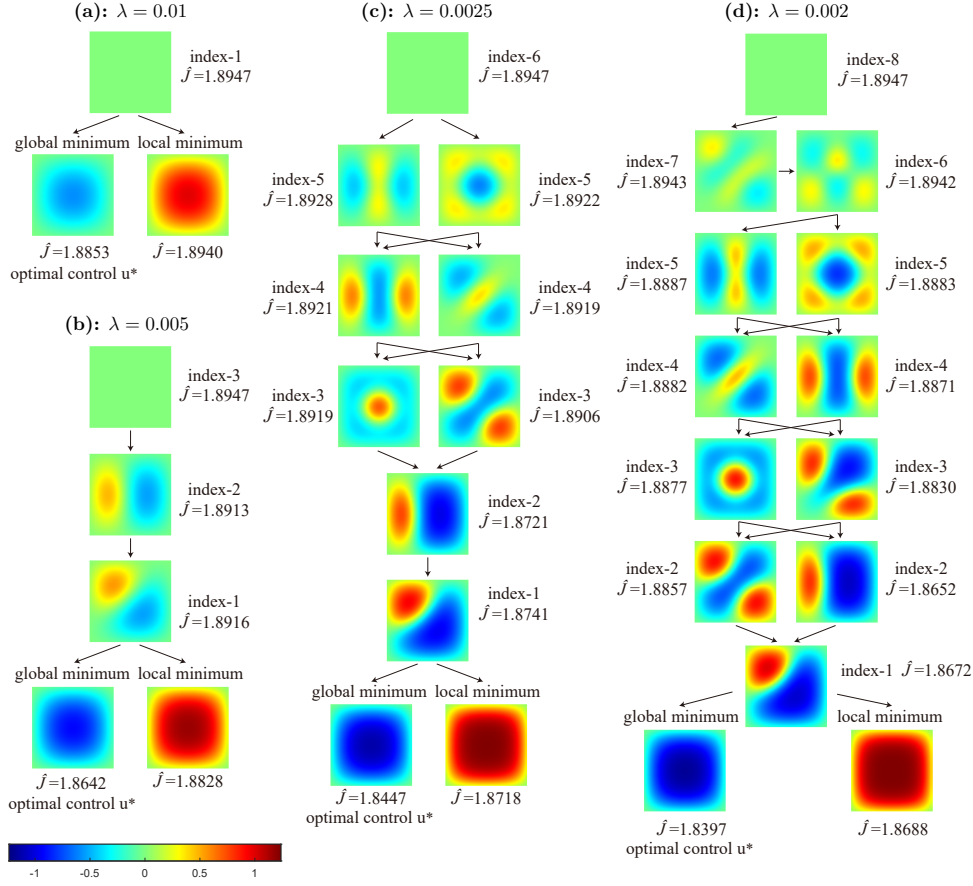


Fig. 4: Control landscapes of asymmetric and unconstrained case 2 with $\lambda = 0.01, 0.005, 0.0025, 0.002$.

constraint the constrained problem (3.10)–(3.11) admits a unique optimal control. The distribution of optimal control has a sharp interface due to the integral constraint, which is different to the unconstrained case. Numerical results again demonstrate the effectiveness of the control landscape in solving constrained optimal control and the applicability of the idea of imposing the constraint on PCHiSD.

5. Concluding remarks. In this work, we solve the non-convex optimal control by using PCHiSD and constructing the control landscape, which could locate local and global minima without requiring good initial guesses. Numerical results indicate the strength of the control landscape in solving the non-convex optimal control. It is worth mentioning that though the current work focuses on an optimal control of elliptic equation, the proposed idea has a great universality and could be widely extended to other optimal control and optimization problems. For instance, optimal control with different cost functionals subject to different PDEs and admissible sets could be considered, though some details still need further exploration, e.g. how to ensure that the state variable of HiSD evolves in the admissible set is not a trivial

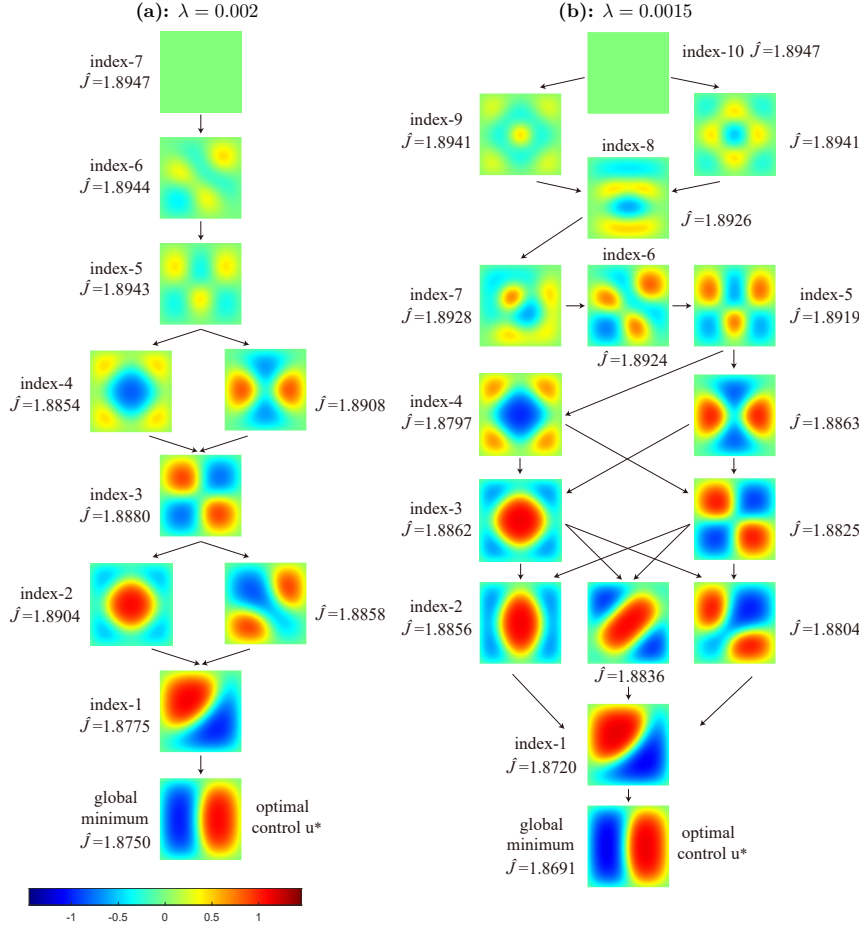


Fig. 5: Control landscapes of asymmetric and constrained case 3 with $\lambda = 0.002, 0.0015$.

issue. Furthermore, the control landscape contains much more information than the location of minima, and numerical results reveal rich solution structures of the non-convex optimal control. Whether these information have physical meanings with possible applications remains further study.

REFERENCES

- [1] A. AHMAD ALI, K. DECKELNICK, AND M. HINZE, *Global minima for semilinear optimal control problems*, Comput. Optim. Appl., 65 (2016), pp. 261–288.
- [2] A. T. BARKER, T. REES, AND M. STOLL, *A fast solver for an H^1 regularized PDE-constrained optimization problem*, Commun. Comput. Phys., 19 (2016), pp. 143–167.
- [3] J. BARZILAI AND J. M. BORWEIN, *Two-point step size gradient methods*, IMA J. Numer. Anal., 8 (1988), pp. 141–148.
- [4] L. BETZ, *Optimal control of a non-smooth elliptic PDE with non-linear term acting on the control*, Math. Control Relat. Fields, (2025), <https://doi.org/10.3934/mcrf.2025032>.
- [5] E. CASAS AND M. MATEOS, *Optimal control of partial differential equations*, Springer International Publishing, Cham, 2017, pp. 3–59.

- [6] E. CASAS AND F. TRÖLTZSCH, *On optimal control problems with controls appearing nonlinearly in an elliptic state equation*, SIAM J. Control Optim., 58 (2020), pp. 1961–1983.
- [7] Y. CHEN, N. YI, AND W. LIU, *A Legendre–Galerkin spectral method for optimal control problems governed by elliptic equations*, SIAM J. Numer. Anal., 46 (2008), pp. 2254–2275.
- [8] I. CHRYSOVERGHI AND J. GEISER, *Descent-penalty methods for relaxed nonlinear elliptic optimal control problems*, in Large-Scale Scientific Computing, I. Lirkov, S. Margenov, and J. Waśniewski, eds., Berlin, Heidelberg, 2008, Springer, pp. 300–308.
- [9] C. CLASON, K. ITO, AND K. KUNISCH, *A convex analysis approach to optimal controls with switching structure for partial differential equations*, ESAIM Control Optim. Calc. Var., 22 (2016), pp. 581–609.
- [10] C. CLASON, A. RUND, AND K. KUNISCH, *Nonconvex penalization of switching control of partial differential equations*, Syst. Control Lett., 106 (2017), pp. 1–8.
- [11] J. COLETSOS AND B. KOKKINIS, *Optimal control of nonlinear elliptic PDEs – theory and optimization methods*, in Large-Scale Scientific Computing, I. Lirkov, S. Margenov, and J. Waśniewski, eds., Berlin, Heidelberg, 2014, Springer, pp. 81–89.
- [12] Y. DAI, B. JIN, R. C. SAU, AND Z. ZHOU, *Solving elliptic optimal control problems via neural networks and optimality system*, Adv. Comput. Math., 51 (2025), p. 31.
- [13] Y. DENG, P. MEHLITZ, AND U. PRÜFERT, *On an optimal control problem with gradient constraints*, Optimization, 69 (2020), pp. 519–551.
- [14] Y. DENG, P. MEHLITZ, AND U. PRÜFERT, *Coupled versus decoupled penalization of control complementarity constraints*, ESAIM Control Optim. Calc. Var., 27 (2021), p. 45.
- [15] L. C. EVANS, *Partial differential equations*, vol. 19 of Graduate Studies in Mathematics, American Mathematical Society, Providence, RI, 2nd ed., 2010.
- [16] W. GONG, Z. TAN, AND Z. ZHOU, *Optimal convergence of finite element approximation to an optimization problem with PDE constraint*, Inverse Probl., 38 (2022), p. 045004.
- [17] L. GUO AND J. J. YE, *Necessary optimality conditions for optimal control problems with equilibrium constraints*, SIAM J. Control Optim., 54 (2016), pp. 2710–2733.
- [18] M. HINZE, R. PINNAU, M. ULBRICH, AND S. ULBRICH, *Optimization with PDE constraints*, vol. 23 of Mathematical Modelling: Theory and Applications, Springer Netherlands, Dordrecht, 2009.
- [19] B. T. KIEN, A. RÖSCH, N. H. SON, AND N. V. TUYEN, *FEM for semilinear elliptic optimal control with nonlinear and mixed constraints*, J. Optim. Theory Appl., 197 (2023), pp. 130–173.
- [20] W. LIU AND N. YAN, *A posteriori error estimates for control problems governed by nonlinear elliptic equations*, Appl. Numer. Math., 47 (2003), pp. 173–187.
- [21] P. MERINO AND A. NENJER, *Numerical approximation of regularized non-convex elliptic optimal control problems by the finite element method*, <https://doi.org/10.48550/arXiv.2209.11384>.
- [22] J. MILNOR, *Morse Theory*, Princeton University Press, Princeton, NJ, 2016.
- [23] J. NOCEDAL AND S. J. WRIGHT, *Numerical optimization*, Springer Series in Operations Research and Financial Engineering, Springer New York, 2006.
- [24] F. TRÖLTZSCH, *Optimal control of partial differential equations*, vol. 112 of Graduate Studies in Mathematics, American Mathematical Society, Providence, Rhode Island, Apr. 2010.
- [25] W. WANG, L. ZHANG, AND P. ZHANG, *Modelling and computation of liquid crystals*, Acta Numer., 30 (2021), pp. 765–851.
- [26] Z. XU, Y. HAN, J. YIN, B. YU, Y. NISHIURA, AND L. ZHANG, *Solution landscapes of the diblock copolymer-homopolymer model under two-dimensional confinement*, Phys. Rev. E, 104 (2021), p. 014505.
- [27] J. YIN, Z. HUANG, AND L. ZHANG, *Constrained high-index saddle dynamics for the solution landscape with equality constraints*, J. Sci. Comput., 91 (2022), p. 62.
- [28] J. YIN, B. YU, AND L. ZHANG, *Searching the solution landscape by generalized high-index saddle dynamics*, Sci. China Math., 64 (2021), pp. 1801–1816.
- [29] J. YIN, L. ZHANG, AND P. ZHANG, *High-index optimization-based shrinking dimer method for finding high-index saddle points*, SIAM J. Sci. Comput., 41 (2019), pp. A3576–A3595.
- [30] L. ZHANG, P. ZHANG, AND X. ZHENG, *Understanding high-index saddle dynamics via numerical analysis*, Commun. Math. Sci., 23 (2025), pp. 541–560.
- [31] L. ZHANG, X. ZHENG, AND S. ZHU, *Numerical analysis for computing multiple solutions of semilinear elliptic problems by high-index saddle dynamics: Part I–Index-1 case*, <https://doi.org/10.48550/arXiv.2508.01534>.
- [32] L. ZHANG, X. ZHENG, AND S. ZHU, *Numerical analysis for computing multiple solutions of semilinear elliptic problems by high-index saddle dynamics: Part II–Index-k case*, submitted.